Author/s:
Palmieri, G;Rinaldi, A;Campagnolo, L;Tortora, M;Caso, MF;Mattei, M;Notargiacomo, A;Rosato, N;Bottini, M;Cavalieri, F

Title:
Hyaluronic Acid Nanoporous Microparticles with Long In Vivo Joint Residence Time and Sustained Release

Date:
2017-06-01

Citation:
Palmieri, G., Rinaldi, A., Campagnolo, L., Tortora, M., Caso, M. F., Mattei, M., Notargiacomo, A., Rosato, N., Bottini, M. & Cavalieri, F. (2017). Hyaluronic Acid Nanoporous Microparticles with Long In Vivo Joint Residence Time and Sustained Release. Particle and Particle Systems Characterization, 34 (6), https://doi.org/10.1002/ppsc.201600411.

DOI: 10.1002/ ((please add manuscript number))

Article type: Full Paper

Hyaluronic Acid Nanoporous Microparticles with Long *in vivo* Joint Residence Time and Sustained Release

Graziana Palmieri, Antonio Rinaldi, Luisa Campagnolo, Mariarosaria Tortora, Maria Federica Caso, Maurizio Mattei, Andrea Notargiacomo, Nicola Rosato, Massimo Bottini, and Francesca Cavalieri**

Dr G. Palmieri, Prof. M. Mattei, Centre for Interdepartmental Services and Animal Technology, University of Rome Tor Vergata, Rome, Italy.

Dr. A. Rinaldi, SSPT Sustainability Department, ENEA, Rome, Italy.

Dr. L. Campagnolo, Department of Department of Biomedicine and Prevention, University of Rome Tor Vergata, Rome, Italy.

Dr. M. Tortora, Dr. F. Cavalieri, Dipartimento di Scienze e Tecnologie Chimiche, Universita' di Roma Tor Vergata, Rome, Italy.

Dr M. F. Caso NANOFABER srl, Via G.A. Badoero, 82 – 00154 Rome, Italy

Dr. A. Notargiacomo, Institute for Photonics and Nanotechnology, CNR, Rome, Italy.

Prof. N. Rosato, Prof. M. Bottini, Department of Experimental Medicine and Surgery, University of Rome Tor Vergata, Rome, Italy. E-mail massimo.bottini@uniroma2.it

Prof. M. Bottini, Infectious and Inflammatory Diseases Research Center, Sanford Burnham Prebys Medical Discovery Institute, La Jolla, CA, USA.

Dr. F. Cavalieri, Department of Chemical and Biomolecular Engineering, The University of Melbourne, Parkville, Victoria 3010, Australia. E-mail:francesca.cavalieri@unimelb.edu.au;

Keywords: Hyaluronic acid, nanoporous particles, microsponges, intra-articular injections.

We report on a relatively simple approach to engineer biodegradable and biocompatible nanoporous hyaluronic acid particles (NPHAs) with a characteristic sponge-like morphology and uniform size. These NPHAs can be synthesized using the concomitant crosslinking of hyaluronic acid and the cross-linking agent precipitation. The nanoporous architecture of NPHAs prevents the rapid enzymatic degradation of hyaluronic acid and controls the erosion of microparticles in physiological conditions. Once injected into an intra-articular body cavity of healthy mice, these NPHAs reside at the point-of-delivery for an extended time period exhibiting a sustained release of hyaluronic acid. In addition, *in vivo* studies indicated the persistence of NPHAs in the knee joints with neither accumulation into major organs, nor any local or systemic side-effect. We emphasize the use of NPHAs as reservoirs of hyaluronic acid, effectively providing an innovative and safe platform for prolonging the favorable effects displayed by hyaluronic acid on joints affected by osteoarthritis.

1. Introduction

Hyaluronic acid (HA) is an important building block of articular cartilage and synovial fluid (SF), which primarily controls the viscoelasticity and rheology of SF [1]. Endogenous HA is synthesized and released into the joint space by fibroblast-like synoviocytes. Because the concentration and molecular weight of HA is reduced in osteoarthritic (OA) joints, the injection of exogenous HA within affected joints represents an FDA-approved treatment to replenish this macromolecule and restore the physiological viscoelastic properties of the synovial fluid. Several different formulations of crosslinked and not-crosslinked HA solutions, with varying composition and molecular weight, are clinically available for intra-articular injection [2-5]. Such HA viscous solutions are indicated to address symptomatic pain in OA patients that are refractory to non-pharmacologic treatments. Yet, HA solutions have a dwell time in the joint of 12-24 hours due to rapid egress of injected solutions *via* synovial capillaries and lymphatic systems[6,7]. Recent *in vivo* studies showed that the joint half-life of very high molecular weight or crosslinked hyaluronate preparations can be prolonged up to 48 hours [6]. The rapid egress of HA formulations from the joint cavity negatively impacts their efficacy in reducing pain in OA patients. Consequently, multiple injections per year are required to provide a prolonged and stable pain relief. However, frequent injections increases patient discomfort and the risk of infections. Overall these facts emphasize the need for the development of biomaterials platforms, such as HA microparticles, that may enable the sustained release of HA over a period of several weeks, or even months, after a single intra-articular (IA) injection. Cross-linked solid (non-porous) HA micro- and nanospheres are generally prepared by a water-in-oil emulsion crosslinking technique, using mineral oil or organic solvents as continuous phase, and requiring many purification

steps to remove the organic solvents [8-10]. Alternatively, non-porous HA microspheres can be obtained by using spray-drying methods [11]. Nevertheless, current manufacturing technology of HA particles offers limited control of particle degradation kinetics, size, porosity, shape and/or surface chemistry [12]. Thus, methods to prepare injectable HA porous microparticles displaying slow sustained HA release, controlled size and mechanical properties, are desirable to develop efficient approaches for pain relief and functional improvements in OA treatment. Furthermore, injectable HA microparticles can be engineered to deliver therapeutic agents into the joint space [13-16]. In this respect, the nanopores can accommodate biotherapeutics, as well as nanoparticles. Herein, we report a simple approach to engineer biodegradable and biocompatible sponge-like HA particles, (NPHAs),endowed with a nanoporous structure. Such NPHAs can be synthesized using a one-pot self-precipitation process induced by the intermolecular and intramolecular crosslinking of HA without using organic solvents. In this study, we demonstrate that the NPHAs are biodegradable, responsive to a reducing agent and exhibit a sustained HA release under both redox and enzymatic treatment. Through *in vivo* investigations in healthy mice, the NPHAs are observed to persist in the knee joints for up to five weeks following IA injection, while neither accumulating into any major organ nor eliciting any local or systemic side-effect. Based on our investigation, we suggest that these NPHAs may provide an innovative and safe biomaterials platform to advance in OA treatment by prolonging the favorable effects of HA over unprecedented duration after injection in a joint.

2. Results and Discussion

2.1 Synthesis and characterization of NPHAs.

NPHAs were prepared using a self-precipitation/crosslinking technique (**Figure 1**). First, the crosslinker was prepared by coupling 1,1 carbonyldiimidazole (CDI) to cystamine. This one-pot reaction of carbonylimidazolide in water at room temperature with a nucleophile was recently developed by Padiya *et al* [17] and provides an efficient method for the preparation of carbamate crosslinkers without using anhydrous solvents in inert atmosphere. CDI, though unstable in water, rapidly reacts with cystamine at room temperature to give a stable bis-carbonylimidazolide crosslinker. Next, HA solution (1% w/v) was mixed with the bis-carbonylimidazolide in aqueous solution and kept under constant shaking overnight. NPHAs were obtained by precipitation of the viscous and high molecular weight HA solution induced by intramolecular and intermolecular crosslinking.

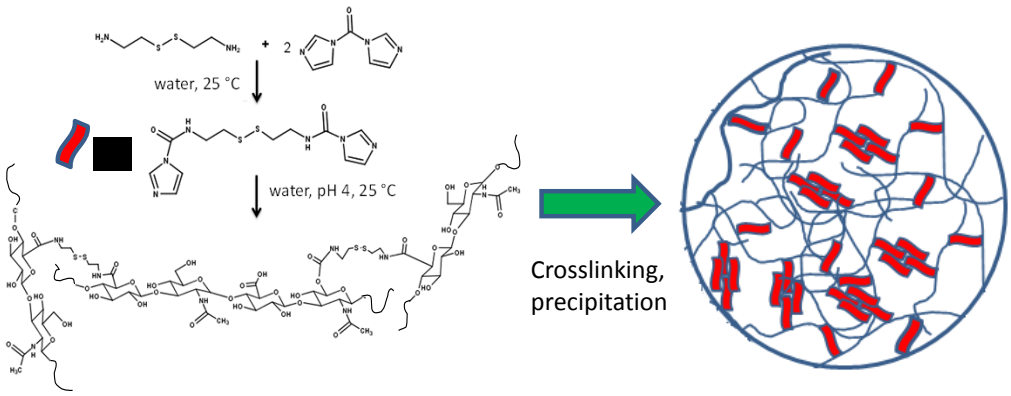

Figure 1. Scheme of preparation of bis-carbonylimidazolide cross-linker and crosslinked porous NPHAs. NPHAs were obtained mixing a high molecular weight HA solution and the CDI activated crosslinker. In addition, HA acts as backbone for nucleation and crystallization of the cross-linking agent.

A control experiment was performed dissolving the prepared crosslinker in aqueous solution without HA. A precipitate composed of large and irregular particles formed after 24 hours (**Figure S1a**). These results suggest that in addition to react with the cross-linking agent through its hydroxyl and carboxyl groups, the HA chains serve as backbone for nucleation and crystallization of the cross-linking agent. To investigate and confirm the structural, chemical and functional properties of NPHAs, the particles were labelled with either fluorescein isothiocyanate (FITC-NPHAs) or near-infrared (NIR)-emitting fluorochromes (NPHA-750).

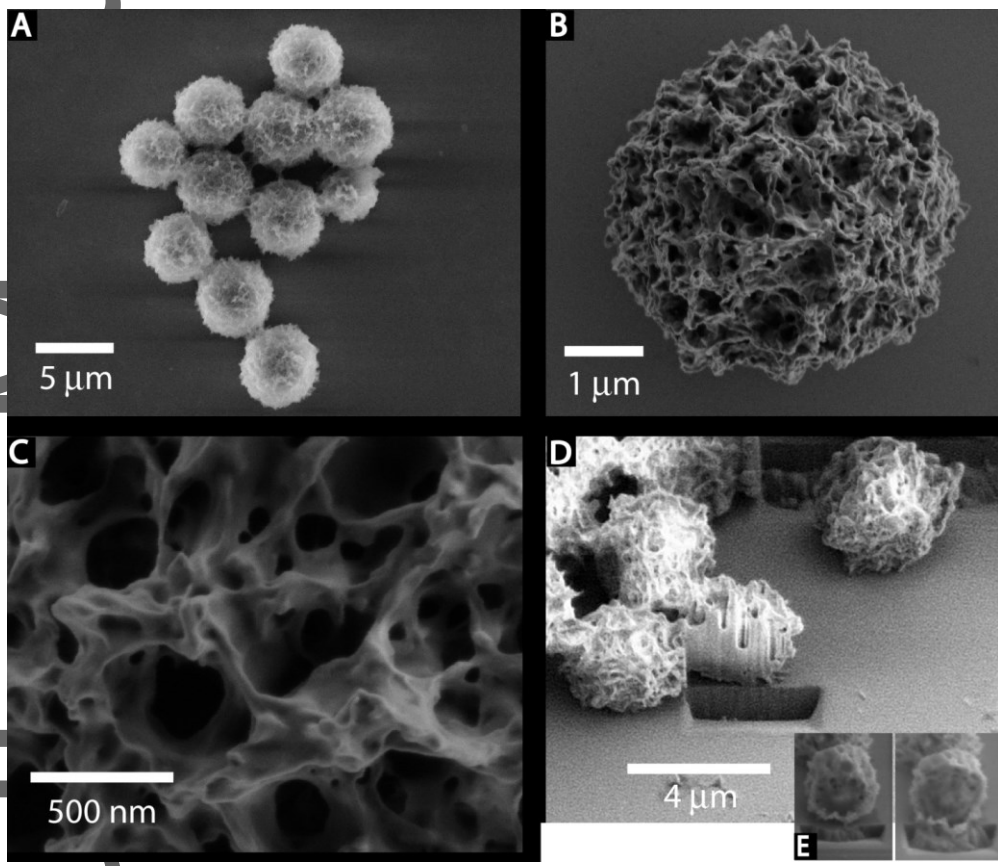

Figure 2. Low-voltage FEG-SEM micrograph (taken at 500V) of NPHAs. A) Representative FEG-SEM images of NPHAs displaying the nanoporous structure; B) and C) Higher magnification SEM images (at 500V) enabled the evaluation of the distribution of NPHA pore size. D) Dual-beam focused ion beam (FIB) cross-section analysis was used to investigate the morphology of particle inner core; E) two snapshots of the serial cross-sectioning through the middle of a 3 μm NPHA.

The resulting NPHAs were spherical in shape and porous. Scanning electron microscope (SEM) micrographs clearly display the NPHAs porous structure (**Figure 2A-2C**). The pore diameters were measured for 100 dry particles and showed a distribution centered at approximately 200±70 nm, which makes NPHAs potentially accessible to biomolecules or even nanoparticles. The nanoporosity can be attributed to two possible reasons: (i) the reaction of the crosslinker with glucuronic acid moieties produces CO_2, which likely acts as porogen agent and leads to the formation of nanopores within the matrix of a particle, (ii) HA functional groups provide a location for the nucleation of the primary crosslinker crystals and large agglomerates of HA molecules and crosslinker crystals are subsequently formed (**Figure 1**). We speculate that the polymer backbone induces the nucleation of the crosslinker crystals to form the scaffold for the particles and serves as a 'glue' to slowly bind the agglomerates together. Indeed, this evokes the mechanism of formation of protein-inorganic hybrid nanoflowers [18, 19] and it is corroborated by the Maltese-cross pattern observed for NPHAs using cross-polarization microscopy (**Figure S1b**) which indicate the formation of crystalline domains embedded into the nanoporous microparticles. The nanoporosity endowed NPHAs with swelling capability in aqueous environments. The diameter of dry (3.3±0.9 μm, N=200) and water-swollen (4.2±0.9 μm, N=200) NPHAs were measured for particles imaged by means of a field-emission SEM

and a confocal microscope, respectively **(Figure 2A and 3A**). The moderate swelling capability of NPHAs suggests a highly crosslinked structure.

To investigate the inner morphology of NPHAs and rule out possible core-shell structure, the NPHAs were cross-sectioned by focused ion beam (FIB), which showed a homogeneous solid core (**Figure 2D**) and a porous outer shell. The surface morphology of NPHAs was assessed at the nanoscale by measuring the surface roughness for dry and water-swollen particles by means of atomic force microscopy (AFM). These measurements (**Figure. 3C and 3D**) showed a significant difference between dry (RMS_{DRY} = 92.8±1.6 nm) and water-swollen particles (RMS_{WET} = 13.8±3.4 nm), thus suggesting that the particle surface stretched and smoothened upon hydration. Three-dimensional reconstruction of confocal microscopy images showed that hydrated NPHAs deformed under coverslip pressure, which suggested particle deformability (**Figure 3B**). The deformability and stiffness of NPHAs was further studied on particles in dry state by means of a single particle micro-compression tests.

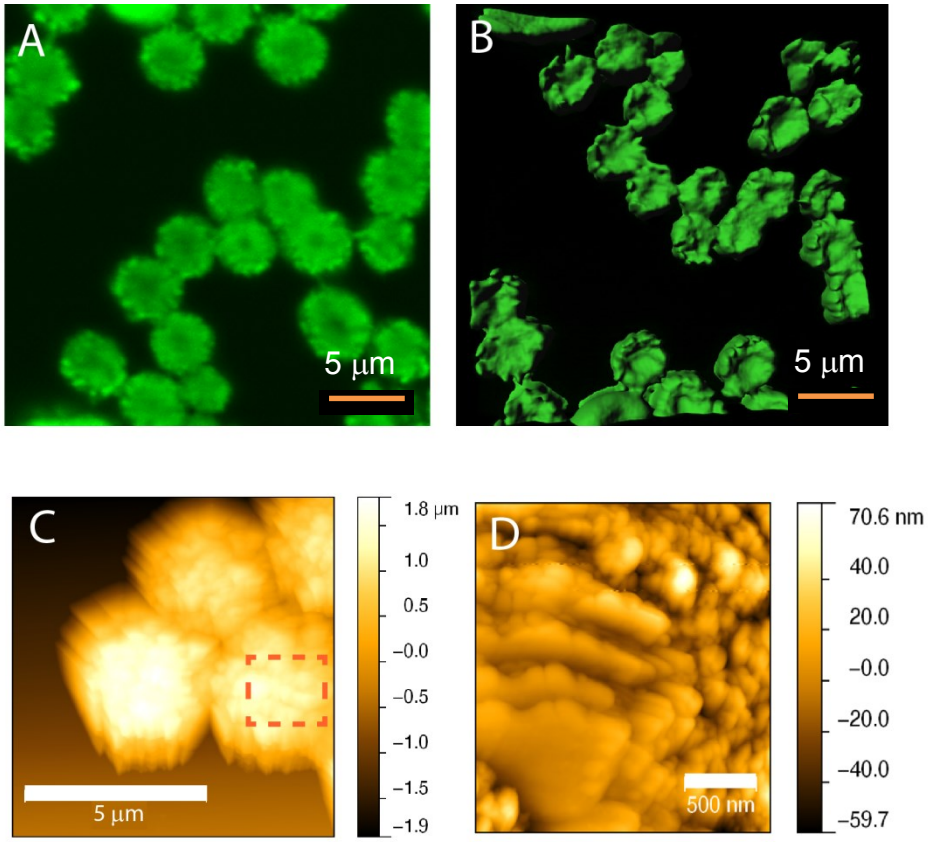

Fig. 3. Confocal microscope and AFM imaging of NPHAs. A) Representative confocal microscope image of water-swollen NPHAs labelled with FITC. The image shows a porous surface upon hydration. B) Three dimensional reconstruction of confocal optical planes shows deformed NPHAs under coverslip pressure. C) and D) AFM images of dry (C) and water-swollen (D) NPHAs were used to evaluate particle surface roughness. The surface of water-swollen NPHAs was smoother than that of dry particles, suggesting surface stretchability.

These measurements showed a substantial elastic recovery upon unloading and an apparent Young's modulus of 25.5 ± 0.5 MPa (**Figure 4**). It has been described that the Young's modulus of crosslinked polymeric particles can be largely tuned (i.e. from kilo to mega Pascals) by changing the cross-linker concentration, the polymer chemical composition and the particle hydration state [20, 21]. The high Young's modulus of our NPHAs suggests a stiff core due to the presence of crystalline domains, thus confirming the observation from cross-polarization microscopy analysis (**Figure S1b**).

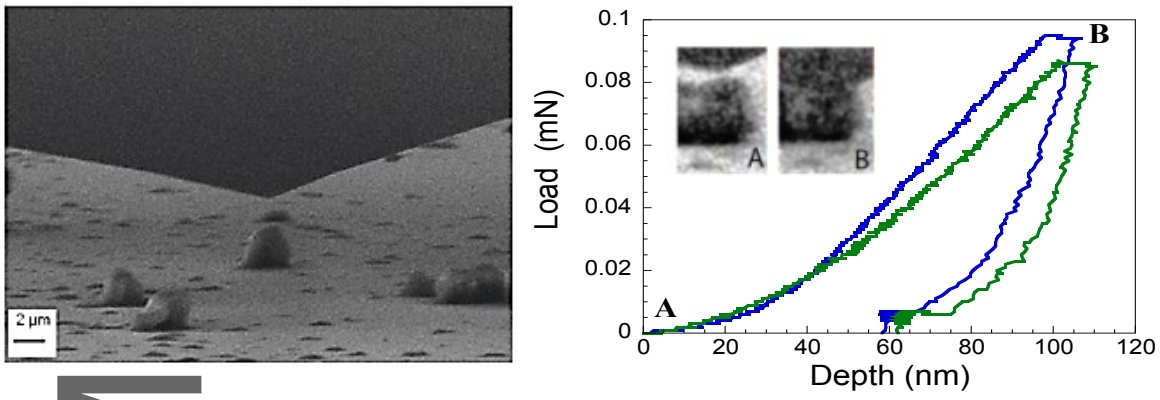

Figure. 4. *In-situ* nanomechanical testing of single NPHAs. Overview of Berkovitch diamond tip hanging over a target NPHA in a SEM-monitored nanoindentation system (left) and resulting load *vs* depth curves associated to gentle compression (100nm depth) from two distinct NPHAs with a diameter of approximately 3 µm (right). The inset shows image frames captured before tip engagement (A) and at maximum load (B), providing visual confirmation of test validity.

2.2 Degradation kinetics of NPHAs.

To verify the ability of NPHAs to disassemble upon redox or enzymatic treatment, FITC-labelled particles (FITC-NPHAs) were incubated in PBS at 37 °C either with 10 mM of reducing agent dithiothreitol (DTT) or with 100 U/mL (pH 7.4) of hydrolytic enzyme hyaluronidase, respectively. The fluorescence of the soluble supernatant, after centrifugation of non-degraded particles, was monitored over time (**Figure 5**). The complete disassembly of NPHAs by DTT occurred within 8 hours (**Figure 5A**).

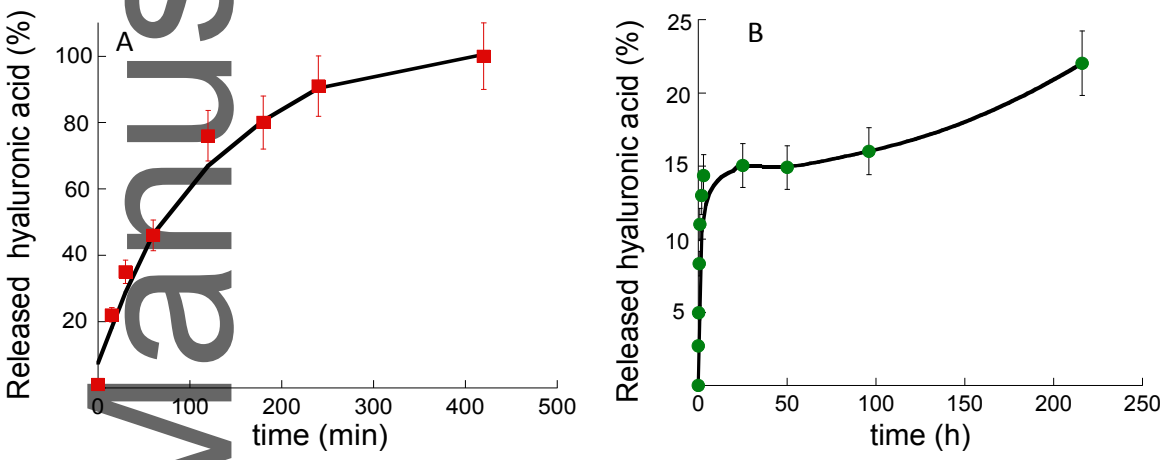

Figure 5. Degradation kinetics of NPHAs. A) Kinetics of release of FITC-HA from NPHAs exposed to 10 mM DTT in PBS at 37 °C. A complete deconstruction of NPHAs is observed after approximately 8 hours. B) Degradation kinetics of NPHAs treated with hyaluronidase (100 U/mL at pH 7.4) at 37 °C.

The supernatant fluorescence *vs* time curve exhibited a plateau, indicating that the redox disassembly process of NPHAs into high molecular weight HA chains was completed. This was confirmed by the absence of residual NPHAs in the vials after the last centrifugation. In addition, the deconstruction of NPHAs into soluble HA by cleavage of disulphide bonds confirms that NPHAs were stabilized by the crosslinker. Conversely, the enzymatic degradation of NPHAs upon enzymatic treatment was not complete, even after several days of incubation with lytic enzyme. Although free HA chains were promptly hydrolyzed by hyaluronidase within few hours (data not shown), only 22 % (w/w) of the HA was released after 9 days of NPHA incubation with hyaluronidase (**Figure 5B**). The initial burst release (15%) of HA observed in the supernatant fluorescence *vs* time curve is likely due to the degradation of the swollen and more accessible particle surface. A possible explanation for the observed slow degradation kinetics is that the structural organization of crosslinked and tightly packed HA chains may hinder access of lytic enzymes to polysaccharide binding sites. Overall, these results indicate that NPHAs biodegradation rate is very slow in physiological conditions suggesting a possible use of NPHAs as viscosupplementation agent able to provide a longer pain relief than currently available HA formulations (*e.g.*, Gel-One®) and/or as drug depot displaying a more durable cargo release than other types of polymeric microparticles [22].

2.3 In vivo evaluation of IA-injected NPHAs.

Along with slow biodegradation, slow joint release of IA-injected NPHAs is a fundamental prerequisite for sustained accumulation of HA and/or loaded drugs within the synovial cavity. Hence, we assessed whether NPHAs were able to persist in the synovial cavity of healthy mice over a prolonged period of time. Two groups (N=3) of 3 month-old C57BL/6J (B6) healthy female mice were unilaterally IA-injected with 5 µg of NPHA-750 in 10 µL of PBS or an equivalent amount of

free near infra-red (NIR)-emitting fluorescent probe (Seta750), respectively, in the knee. Whole animals were imaged by means of a Kodak In-Vivo Imaging System FX during the following 2 months (**Figure. 6A** and **Figure S2**) and the intensity of NIR emission arising from treated knees was measured (**Figure 6B**). NIR signal arising from knees treated with a solution of Seta750 became undetectable by our imaging system in less than one day, thus suggesting rapid exit from the synovial cavity of the fluorescent probe *via* synovial capillaries. Conversely, NIR signal arising from NPHA-750-treated knees showed (i) a 2-fold increase in the intensity 1 day after administration, (ii) a slow decrease in the intensity to approximately 10% of the initial value during the following 34 days and (iii) a drop to approximately 1% of the initial value during the following 2 weeks (Figure 6B). The early increase in NIR emission from NPHA-treated knees suggests a change in the environment surrounding NPHA-encapsulated fluorochromes probably due to interaction with synovial fluid proteins following partial disassembling of NPHA matrix. The slow decrease in fluorescence signal over two months suggests that IA-injected NPHAs either escaped from the joints as partially degraded debris *via* the lymphatic system or disassembled into HA chains within the joint cavity which are eliminated by capillary circulation.

Next, we investigated whether the egression of IA-injected NPHAs from the joints led to accumulation into major organs. Two groups (N=2) of 3 month-old B6 healthy female mice were unilaterally IA-injected with 5 μg of NPHA-750 in 10 μL of PBS and sacrificed after 3 days and 2 months, respectively. Two additional groups (N=1) of mice were unilaterally IA-injected with 10 μL of PBS (control). Major organs, including pancreas, spleen, kidneys, liver, lungs, heart and knees were collected and their NIR fluorescence recorded. Three days after injection, liver from both treated animals and kidneys from one treated animal exhibited a weak NIR signal, whereas NIR signals arising from all other extracted organs were undetectable by our imaging system (**Figure 6C**). NIR

signals from all extracted organs were undetectable two months after injection. Overall these results suggest that IA-injected NPHAs left the joints without accumulating into any major organ, indicating a good safety profile.

Finally, although we had shown that IA-injected NPHAs eventually exit the joints without accumulating into any major organ**,** we wanted to rule out that the longer joint persistence time of NPHAs could cause damage to the cartilage *per se*. Therefore, two sets (N=6) of 3 month-old B6 healthy female mice were unilaterally treated in the knee with 5 µg of IA-injected NPHAs in 10 µL of PBS or an equal volume of PBS (control), respectively. Both sets were divided in two groups (N=3) and sacrificed 3 days and 2 months after administration. Treated knees were collected, fixed, decalcified and processed for paraffin embedding. Five micron-thick sections were taken, stained with Hematoxylin and Eosin and imaged by optical microscope (**Figure 6D**). It has been reported that neutrophil infiltration is the primary response to joint inflammation [23] Histological examination of serial sections of the knee joint of animals injected with NPHAs failed to identify the presence of neutrophil infiltration in the joint.. Histologically, mouse neutrophils are easily recognizable due to their ring-shaped nucleus. Overall, we found no damages in cartilage surface of NPHA-treated joints relatively to control knees at both time points, thus validating that our microparticles are possibly an ideal platform for IA sustained-release of HA and/or encapsulated therapeutic agents.

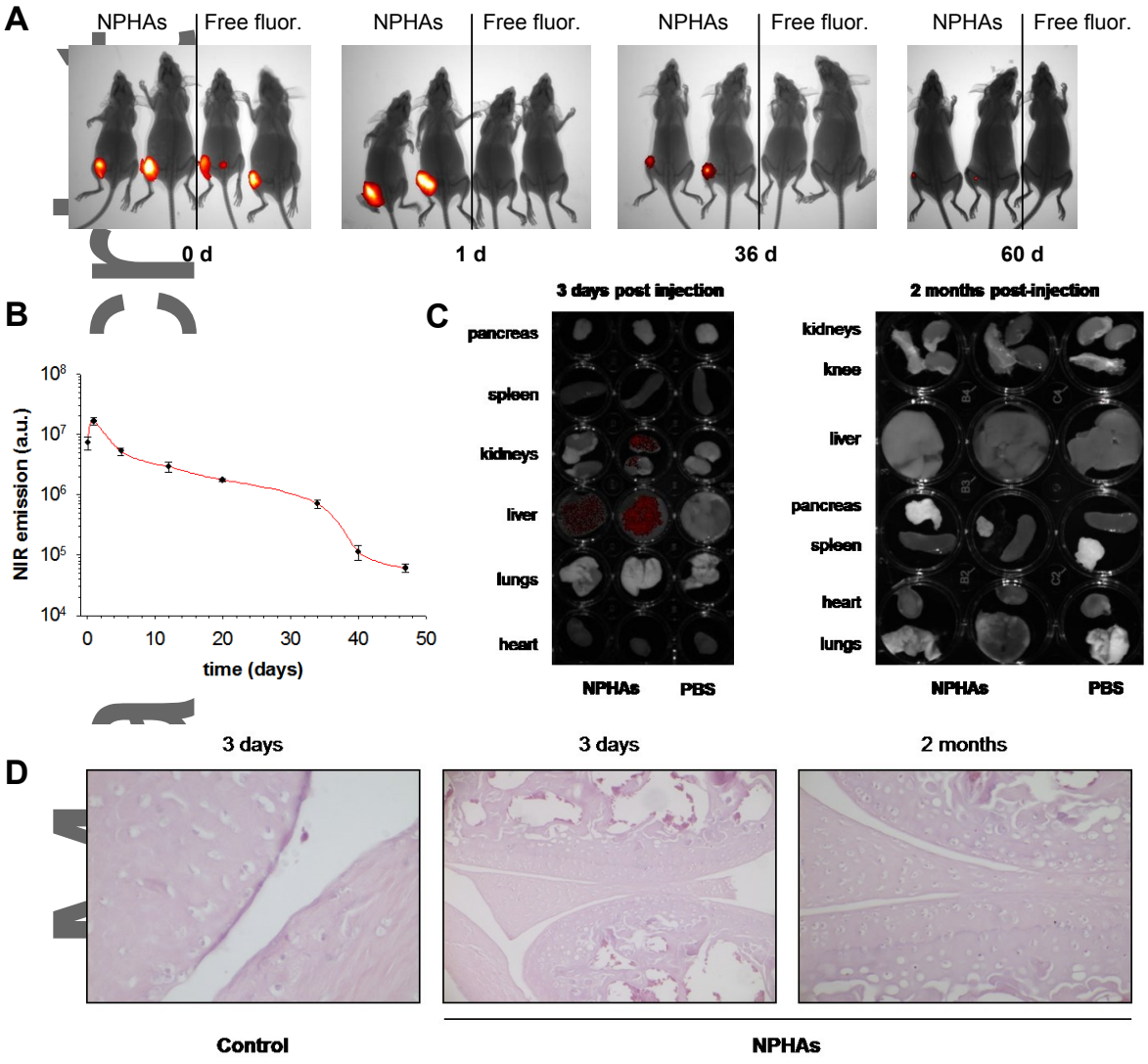

Figure 6 *In vivo* evaluation of IA-injected NPHAs. A and B) Joint persistence time of NPHA-750 and Seta-750. Two groups (N=3) of 3 month-old B6 healthy female mice were unilaterally IA-injected into the knees with 5 µg of NPHA-750 or an equivalent amount of free fluorochrome (Seta750), respectively. NPHA joint residence was monitored by recording the near infra-red (NIR) emission from treated mice through an *in vivo* imaging system (A). NIR emission arising from NPHA-750-

treated knees in function of time. Values are reported as mean ± standard error (B). C) Organ accumulation of IA-injected NPHAs. Two groups (N=2) of 3 month-old B6 healthy female mice were unilaterally IA-injected with 5 µg of NPHAs carrying NIR-emitting fluorochromes (NPHA-750) and sacrificed after 3 days and 2 months, respectively. Two additional groups (N=1) of mice were unilaterally IA-injected with PBS (control). Major organs were collected and their NIR fluorescence recorded. Two months after treatment with NPHAs, no NIR signal was recorded from any of the major organs, thus suggesting that IA-injected NPHAs egressed from joints and were excreted from the body without accumulating into any major organ. D) Effects of IA-injected NPHAs on cartilage integrity. Two sets (N=6) of 3 month-old B6 healthy female mice were unilaterally IA-injected with 5 µg of NPHAs or an equal volume of PBS (control), respectively. Both sets were divided in two groups (N=3) and sacrificed 3 days and 2 months after administration. Treated knees were collected and histologic slides were prepared and stained with Hematoxylin and Eosin. No damages in cartilage surface of NPHA-treated joints relatively to control knees were observed at both time points.

3. Conclusion

Herein we describe the synthesis of biodegradable and biocompatible nanoporous HA microparticles (NPHAs) prepared by self-precipitation and crosslinking of high molecular weight HA in aqueous solution. The simultaneous crosslinking of HA and precipitation of the crosslinker plays a pivotal role in the formation of a nanoporous structure, which is stabilized by crosslinked and tightly packed HA chains, thereby preventing the rapid enzymatic degradation of HA and tuning the erosion of microparticles in physiological conditions. Both *in vivo* and *in vitro* studies consistently demonstrate

the remarkable properties of these NPHAs, highlighting particularly a longer persistence time of up to 5 weeks in murine joints without eliciting any systemic and local side–effects or inducing accumulation into major organs. The potential impact of this promising and safe biomaterial is relevant and manifold, with straightforward translation into clinics for pain relief and functional improvements in OA In addition, NPHAs offers a platform to entrap and slowly release disease modifying OA drugs (DMOADs) aimed at delaying, or even reversing, OA progression. Further efforts are being made for loading DMOADs into the nanopores of NPHAs and modifying their surface with agents targeting specific articular tissues. In fact, the use of targeted HA-based depots can improve the delivery of DMOADs to a specific joint location while reducing injection complications, such as infections, extra-articular injections, and pseudo septic arthritis.

4. Experimental Section

Preparation and characterization of NPHAs: NPHAs were synthesized by a self-precipitation/crosslinking technique. First, the crosslinker was synthesized by dissolving 30 mg of 1,1 carbonyldiimidazole (CDI, Sigma-Aldrich, St. Luis, MO) and 20 mg of cystamine (Sigma-Aldrich) in 200 µL of dry DMSO or MilliQ water. CDI immediately reacts with cystamine to form bis-imidazole-N-carboxamide crosslinker in both DMSO and water. The product precipitated out from the reaction mixture in water at neutral pH and was isolated in pure form by filtration. To dissolve the crosslinker, aqueous solution pH was adjusted to 4 using 1 M HCl. Next, hyaluronic acid (HA, 0.8-1.2 MDa, Sigma-Aldrich) was dissolved in MilliQ under constant stirring overnight. An aqueous HA solution (1% w/v) was mixed with the crosslinker and kept under constant shaking overnight. NPHAs were

obtained by precipitation of the viscous and high molecular weight HA solution induced by intramolecular and intermolecular crosslinking. FITC-labelled HA was used to evaluate the reaction yield by measuring the absorbance of the polymer solution before and after particles precipitation. The experimental yield of HA crosslinking and precipitation was 100 % (w/w). It was experimentally verified that the use of hyaluronic acid with a molecular weight lower than that 1 MDa fails to achieve a uniform spherical structure and requires longer reaction times, whereas the use of hyaluronic acid with a molecular weight greater than 1 MDa leads to an increase in the viscosity of the hyaluronic acid solution, with resulting inhomogeneity of the reactive mixture. It was also experimentally found that, if the hyaluronic acid has a concentration lower than 0.5 % w/v, the resulting micro-sponges are not uniform, whereas, if the hyaluronic acid has a concentration greater than 1 % w/v, the resulting solution is too viscous, thus preventing the formation of uniform microparticles. The concentration of the crosslinker was optimized to control the kinetics of crystallization and consequently the formation of uniform micrometer sized particles. HA microsponges were recovered by centrifugation, washed several times with MilliQ and stored as aqueous suspension at 4°C. NPHAs were labeled with fluorescein isothiocyanate (FITC, Sigma Aldrich) or 750 nm-emitting fluorochromes (NHS-Seta750, Ex 752nm/Em 778nm, SETA BioMedicals, Urbana, IL) by following protocols published by the fluorochrome suppliers. The unreacted fluorochromes were removed by repeated washings with Milli-Q water. FITC-labelled particles (FITC-NPHAs) were used to study the morphology of water-swollen particles by means of confocal microscopy (FluoView 1000 LSCM system, Olympus, Tokyo, Japan), whereas Seta750-labelled particles (NPHA-750) were used for particle tracking in living animals by means of a Kodak In-Vivo Imaging System FX (Carestream Health, Inc., Rochester, NY). The concentration of NPHAs was determined using a microscope counting chamber hemocytometer. Surface morphology of NPHAs "as is" (*i.e.*, without any sputter coating) were observed by means of a scanning electron microscope (SEM, model Leo Supra-35, Carl Zeiss Microscopy GmbH, Jena,

Germany) and an atomic force microscope (AFM, model Flex-FPM, NANOSURF, Liestal, Switzerland). SEM was used at a low accelerating voltage of 0.5-2 kV to reduce damages to the NPHAs. The NPHAs' inner structure was studied by cross-sectioning and imaging the particles by means of a dual-beam focused ion beam (FIB, model Helios NanoLab™ DualBeam™, FEI, Hillsboro, OR) equipped with a Ga^+ liquid metal ion source. Particles were milled by focused ion beam at 30kV acceleration voltage and 280pA current. A final step at a current of 48pA was performed to obtain a smooth and polished surface. Cross section view images were collected by SEM at a 52º tilt angle, 170pA current and 2kV acceleration voltage. AFM measurements were performed in non-contact mode on scanning areas up to 50×50 μm^2 to assess surface homogeneity and roughness of particles. Samples were observed in both dry (standard in-air AFM) and water-swollen (in-liquid AFM) conditions using the same set of cantilevers with aligning grooves and spring constant of 48 N/m (A190G, Budget Sensors®, Sofia, Bulgaria). For in-liquid AFM, the particles were hydrated with nano-pure water and scanned using a cantilever mount with a refraction-index corrected glass that allows monitoring the immersed tip by a camera. The cantilever resonant frequency was ~190 KHz and ~80 KHz in air and liquid, respectively. Root Mean Square (RMS) roughness was calculated using GWYDDION software (v.2.38, gwyddion.net, Czech Republic) on planarized maps of the NPHAs' surface obtained from deconvoluting raw data through a polynomial filter to remove the effect of curvature.

To measure the mechanical response and elastic properties of NPHAs, *in situ* compression tests were performed on single particles by a SEM-monitored nanoindenter (InSEM, Nanomechanics Inc., Oak Ridge, TN) equipped with a Berkovich tip. The effective Young's modulus (E) of NPHAs were calculated by fitting the load *vs* depth curves by an Hertzian model:

$$E = 3D^{1/2}(1-\nu^2)\frac{P}{\delta^{3/2}} \quad (1)$$

where D is the diameter of the particles, P is the applied load , δ is the indentation depth, and ν is the Poisson' s ratio of the material [24-26]. The Hertzian model was used under the assumptions that the curvature of the Berkovitch tip was negligible and the cantilevered tip had a Young's modulus much greater than that of the particles. We used a Poisson's ratio equal to 0.5, which is usually assumed for isotropic incompressible solids and gels.

In vitro degradation of NPHAs: For redox degradation studies, 10 µL of FITC-NPHA suspension in PBS was added to a 10 mM DTT solution and incubated at 37 °C for variable time intervals. At each time point, the suspension of FITC-NPHAs was centrifuged, the supernatant collected and the pellet resuspended in a fresh 10 mM DTT solution. The supernatant was analyzed through a fluorometer to quantify the released FITC-labelled HA fragments. The redox degradation study was carried out for 24 hours. For enzymatic degradation studies, a solution of hyaluronidase (100 U/mL at pH 7.4) was incubated at 37 °C with 50µL of NPHA suspension in PBS at 37 °C. FITC-NPHA suspension was centrifuged, the supernatant collected and the pellet re-suspended in a fresh 100 U/mL hyaluronidase solution. The supernatant was analyzed through a fluorometer to quantify the released FITC-labelled HA fragments. The enzymatic degradation study was carried out for 8 days.

Animal care: Pathogen free 3 month-old C57BL/6J (B6) healthy female mice were purchased from Envigo (Cambridgeshire, United Kingdom). Animals were bred at a temperature of 20±2ºC and a relative humidity of 55±10%. Food (RF21 standard diet, Mucedola s.r.l., Milan, Italy) and water were given *at libitum*. Animals were sedated with a single *s.c.* or *i.p.* dose of anesthetic (Domitor, Pfizer

Inc., New York, NY) before treatment of joints with NPHA-750 for trafficking evaluation or NPHAs for histologic evaluation of particle side-effects, respectively. Animal procedures have been revised and accepted by the internal ethics committee of the Centre for Interdepartmental Services and Animal Technology at the University of Rome Tor Vergata (Decree of the President of the Republic 116/1992). All the *in vivo* procedures were performed by a veterinary surgeon and well trained personnel.

Joint persistence and organ accumulation of NPHAs: Five micrograms of NPHA-750 in 10 μL of PBS or an equivalent amount of free 750 nm-emitting fluorochromes (Seta750) were unilaterally IA-injected into the knees of two groups (N=3) of 3 month-old C57BL/6J (B6) healthy female mice (Envigo, Cambridgeshire, United Kingdom), respectively. Joint residence time of compounds was followed by recording the near infra-red (NIR) emission from treated joints by means of a Kodak In-Vivo Imaging System FX (Carestream Health, Inc.) during the following 2 months. NIR emission was recorded from joints in three different angulations with respect to the light source in order to minimize variability arising from the anisotropic distribution of particles within the joints. Two groups (N=2) of 3 month-old B6 healthy female mice were unilaterally IA-injected with 5 μg of NPHA-750 in 10 μL of PBS and sacrificed after 3 days and 2 months, respectively. Two additional groups (N=1) of mice were unilaterally IA-injected with 10 μL of PBS (control). Major organs (pancreas, spleen, kidneys, liver, lungs, heart and knees) were extracted and their NIR fluorescence recorded.

Histological evaluation of NPHA in vivo effects: Two sets (N=6) of 3 month-old B6 healthy female mice were unilaterally IA-treated in the knee with 5 μg of NPHAs in 10 μL of PBS or an equal

volume of PBS (control), respectively. The sets were divided in two groups (N=3) and sacrificed 3 days and 2 months after administration, respectively. Knees were collected, fixed in 10% neutral buffered zinc-formalin for 2 days, decalcified for 4 days in Cal-Ex II solution (Thermo Scientific, Rockford, IL) and processed for paraffin embedding using standard protocols. Five micron-thick sections were obtained with a microtome (Leica Biosystems, Inc., Buffalo Grove, IL) from each knee, stained with Hematoxylin and Eosin and imaged by optical microscope.

Supporting Information

Supporting Information is available from the Wiley Online Library or from the author.

Figure S1: Optical microscopy images of the crosslinker precipitate and cross-polarization microscopy image of NPHAs. Figure S2: *In vivo* evaluation of IA-injected NPHAs from 0 d to 60 d.

Acknowledgements

This work was supported by the ARC Future Fellowship (t F. C. project number FT140100873) and the John Vaughan Scholarship from the Arthritis National Research Foundation (M.B.). We thank I. Mella, G. Menna, A. Mirardi, and L. Quadrini (University of Rome Tor Vergata) for experimental support. The authors have no conflicts of interest to declare.

‡G.P. and A.R. contributed equally to this work

REFERENCES

[1] T.M. Tamer, *Interdiscip. Toxicol.*, **2013**, *6*, 111.

[2] E. Ayhan, H. Kesmezacar, I. Akgun, *World J. Orthop*. **2014**, *5*, 351.

[3] A. Fakhari, C. Berkland, *Acta Biomater.,* **2013***, 9*, 7081.

[4] J. Li, D. J Gorski, W. Anemaet, J. Velasco, J. Takeuchi, J. D. Sandy, A. Plaas, *Arthritis Res. Ther.* **2012**, *14*, R151.

[5] H. Zille, J. Paquet, C. Henrionnet, J. Scala-Bertola, M. Leonard, J. L. Six; F. Deschamp, P. Netter, J. Vergès, P. Gillet, L. Grossin, *Biomed. Mater. Eng.*, **2010**, *20*, 235.

[6] C.H. Evans, V.B. Kraus, L.A. Setton, *Nat. Rev. Rheumatol*. **2014**, *1*, 11.

[7] M. Bottini, K. Bhattacharya, B. Fadeel, A. Magrini, N. Bottini, N. Rosato, *Nanomedicine*, **2016**, *12*, 255.

[8] Y.H. Yun, D.J. Goetz, P. Yellen, W. Chen, *Biomaterials*, **2004**, *25*, 147.

[9] A.K. Jha, W. Yang, C.B Kirn-Safran, M.C. Farach-Carson, X. Jia, *Biomaterials*, **2009**, *30*, 6964.

[10] L. Messager, N. Portecop, E. Hachet, V. Lapeyre, I. Pignot-Paintrand, B. Catargi, B., R. Auzély-Velty, V. Ravaine, *J. Mater. Chem. B,* **2013**, *1*, 3369.

[11] M. Fatnassi, S. Jacquart, F. Brouillet, C. Rey, C. Combes, S.G. Fullana, *Powder Technology*, **2014**, *255*, 44.

[12] K.M. Chan, R.H. Li, J.W. Chapman, E.M. Trac, J.B. Kobler, S.M. Zeitels, Langer, R.; Karajanagi, S.S. *Acta Biomater.*, **2014**, *10*, 2563.

[13] L. Bédouet, F. Pascale, L. Moine, M. Wassef, S.H. Ghegediban, V.N. Nguyenc, M. Bonneaub, D. Labarree, A. Laurenta, *Int. J. Pharm*., **2013**, *456*, 536.

[14] L.S. Liang, W. Wong, H.M. Burt, *J. Pharm. Sci*., **2005**, *94*, 1204.

[15] R.M. Samarasinghe, R.K. Kanwar, J.R. Kanwar, *Biomaterials*, **2014**, *35*, 7522.

[16] J. Kawadkar, M.K. Chauhan, *Eur. J. Pharm. Biopharm.*, **2012,** *81*, 563.

[17] K.J. Padiya, S. Gavade, B. Kardile, M. Tiwari, S. Bajare, M. Mane, V. Gaware, S. Varghese, D. Harel, S. Kurhad, *Org. Lett.*, **2012**, *14*, 2814.

[18] J. Ge, J. Lei, R. N. Zare, *Nature Nanotech*. **2012**, *7*, 428-432.

[19] S. W. Lee, S. A. Cheon, M. Il Kim, T. J. Park, *J Nanobiotechnol*, **2015**, *13*, 54.

[20] H.K. Heris, M. Rahmat, L. Mongeau, *Macromol. Biosci*., **2012**, *12*, 202.

[21] J.P. Best, J. Cui, M. Müllner, Caruso F. *Langmuir,* **2013***, 29,* 9824.

[22] C. Larsen, J. Ostergaard, S.W. Larsen, H. Jensen, S. Jacobsen, C. Lindegaard C, P.H. Andersen. *J. Pharm. Sci.*, **2008**; *97*, 4622.

[23] H.L. Wright, R.J. Moots, R.C. Bucknall, S.W. Edwards. *Rheumatology (Oxford).* **2010**, *49*, 1618.

[24] P.A Levett, D.W. Hutmacher, J. Malda, T.J. Klein, *PLoS One*, **2012**, *9,* e113216.

[25] F. Cavalieri, J.P. Best, C. Perez, J. Tu, F. Caruso, T. J. Matula, M. Ashokkumar, *ACS Appl. Mater. Interfaces,* **2013***, 5,* 10920.

[26] A. Rinaldi, M.A. Correa-Duarte, V. Salgueirino-Maceira, S. Licoccia, E. Traversa, A.B. Dávila-Ibáñez, A.B., P. Peralta, K. Sieradzki, *Acta Mater*., **2010**, *58*, 6474.

The table of contents entry

Hyaluronic Acid was assembled into nanoporous particles using the polysaccharide backbone for nucleation and crystallization of the cross-linking agent. *In vivo* and *in vitro* studies demonstrate the remarkable functional properties of these nanoporous particles, highlighting a long persistence time of 5 weeks in murine joints without eliciting any systemic and local side–effects or inducing accumulation into major organs.

Keywords: hyaluronic acid, nanoporous particles, microsponges, intra-articular injections.

Graziana Palmieri, Antonio Rinaldi, Luisa Campagnolo, Mariarosaria Tortora, Maria Federica Caso, Maurizio Mattei, Andrea Notargiacomo, Nicola Rosato, Massimo Bottini, and Francesca Cavalieri**

Hyaluronic Acid Nanoporous Microparticles with Long *in vivo* Joint Residence Time and Sustained Release

ToC figure ((Please choose one size: 55 mm broad × 50 mm high **or** 110 mm broad × 20 mm high. Please do not use any other dimensions))